

Review

# Chemical Functionalization of Graphene Nanoplatelets with Hydroxyl, Amino, and Carboxylic Terminal Groups

Cheng Peng and Xiaoyan Zhang \* 

Division of Chemistry and Biochemistry, Department of Chemistry and Chemical Engineering, Chalmers University of Technology, Kemigården 4, SE-412 96 Göteborg, Sweden; chengp@chalmers.se

\* Correspondence: xiaoyan.zhang@chalmers.se; Tel.: +46-317728212

**Abstract:** As the most studied two-dimensional material, graphene is still attracting a lot of attention from both academia and industry due to its fantastic properties such as lightness, excellent mechanical strength, and high conductivity of heat and electricity. As an important branch of graphene materials, graphene nanoplatelets show numerous applications such as in coating, fillers of polymer composites, energy conversion and storage devices, sensing, etc. Chemical functionalization can introduce different functional groups to graphene nanoplatelets and can potentially endow them with different properties and functions to meet the increasing demand in the fields mentioned above. In this minireview, we present an overview of the research progress of functionalized graphene nanoplatelets bearing hydroxyl, amino, and carboxylic terminal groups, including both covalent and noncovalent approaches. These terminal groups allow subsequent functionalization reactions to attach additional moieties. Relevant characterization techniques, different applications, challenges, and future directions of functionalized graphene nanoplatelets are also critically summarized.

**Keywords:** graphene nanoplatelets; hydroxyl group; amino group; carboxylic acid group; covalent and noncovalent functionalization



**Citation:** Peng, C.; Zhang, X. Chemical Functionalization of Graphene Nanoplatelets with Hydroxyl, Amino, and Carboxylic Terminal Groups. *Chemistry* **2021**, *3*, 873–888. <https://doi.org/10.3390/chemistry3030064>

Academic Editor: Michela Alfe

Received: 22 July 2021

Accepted: 18 August 2021

Published: 23 August 2021

**Publisher's Note:** MDPI stays neutral with regard to jurisdictional claims in published maps and institutional affiliations.



**Copyright:** © 2021 by the authors. Licensee MDPI, Basel, Switzerland. This article is an open access article distributed under the terms and conditions of the Creative Commons Attribution (CC BY) license (<https://creativecommons.org/licenses/by/4.0/>).

## 1. Introduction

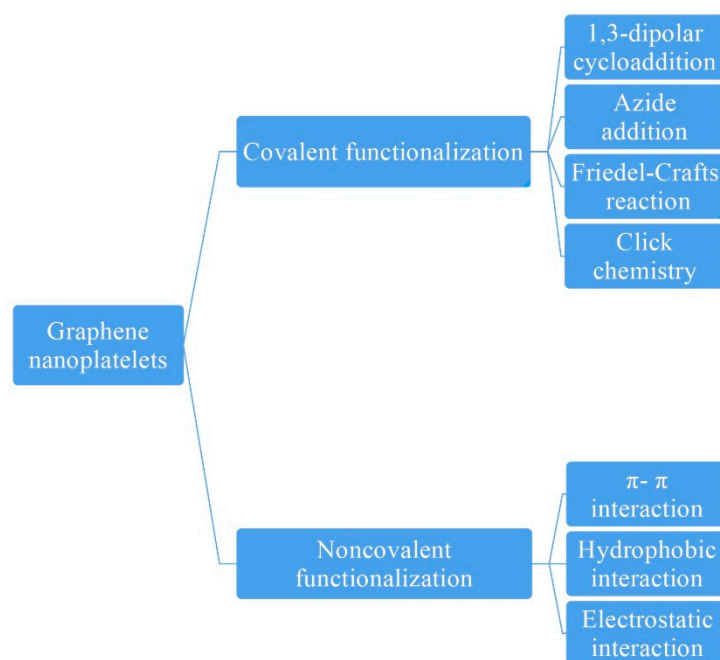
Since the discovery and the groundbreaking research of its electronic properties in 2004 [1], graphene, a one-atom thick layer of  $sp^2$  carbon atoms with a two-dimensional honeycomb lattice, has become one of the most intensively studied materials in chemistry, physics, materials science, and nanotechnology. Graphene is the thinnest and strongest material in the world, and shows an excellent conductivity of heat and electricity. Due to its extraordinary properties, graphene is widely used for electronic devices [2,3], biological applications [4], energy conversion and storage, and nanocomposites [5–7]. To obtain graphene, several common methods, such as scotch-tape cleavage [1], liquid phase/mechanical exfoliation of graphite [8], chemical vapor deposition (CVD) [9,10] and reduction of graphene oxide [11,12], have been developed. Graphene nanoplatelets (GNPs), with a thicknesses of no more than 10 layers and a low content of defects, are an important branch of graphene family. Herein, we mainly discuss the chemical functionalization strategies of GNPs obtained from liquid phase/mechanical exfoliation simply due to their wide usage in industrial production processes.

Due to the strong  $\pi$ - $\pi$  stacking, GNPs are easy to aggregate in solvents, which leads to great challenges during preparation and manufacturing processes. Covalent and noncovalent functionalization of graphene provide a versatile approach to increase the stability of GNPs in solvents, and also can bring new properties by introducing functional groups to GNPs. In this minireview, we aim to summarize the latest development of covalent and noncovalent approaches to introduce amino, hydroxyl, and carboxylic terminal groups onto GNPs, which can increase the dispersibility of GNPs in solvents. Moreover, these terminal groups can also be further functionalized to introduce other interesting functional moieties, which can open a new gate for the further applications of GNPs. Different approaches of the

functionalization of GNPs including 1,3-dipolar cycloaddition, the Friedel–Crafts reaction, nitrene addition, click chemistry, some noncovalent methods, and also the characterization techniques of the functionalized GNPs including X-ray photoelectron spectroscopy (XPS), thermal gravimetric analysis (TGA), infrared spectroscopy (IR), ultraviolet–visible spectroscopy (UV), Raman spectroscopy, transmission electron microscopy (TEM), scanning electron microscope (SEM), atomic force microscopy (AFM), and differential scanning calorimetry (DSC), will be discussed. To the best of our knowledge, there is no such a review summarizing and discussing this specific topic before.

## 2. Covalent and Noncovalent Functionalization of GNPs

Chemical functionalization of GNPs can be classified into two approaches: covalent and noncovalent. The main purpose of functionalization is to increase the dispersibility in different solvents, which is an important step in making GNPs-based nanocomposites and for coating applications. Covalent functionalization can provide a stable connection between the functional group and GNPs. In the meanwhile, introducing functional groups via a covalent approach can also tune the aromatic character of graphene, which can lead to a change in the electronic properties [13]. Different covalent functionalization methods have been developed, generally including the formation of covalent bonds between functional groups and GNPs via reactions such as 1,3-dipolar cycloaddition, azide reaction, the Friedel–Crafts reaction, or click chemistry (Scheme 1).



**Scheme 1.** Functionalization of GNPs using covalent and noncovalent approaches.

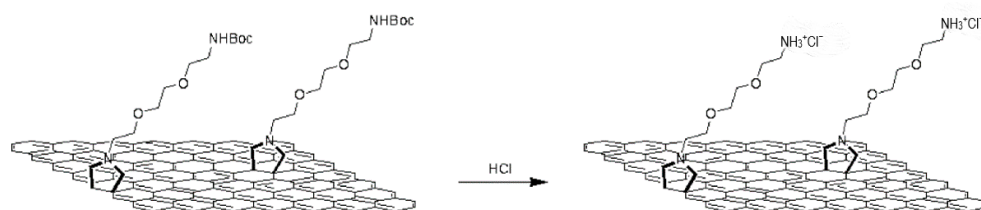
Noncovalent functionalization of GNPs can be achieved by  $\pi$ – $\pi$  stacking as well as hydrophobic or electrostatic interactions [14,15]. For example, the large  $\pi$  system of GNPs can be used as an ideal scaffold for noncovalent functionalization with aromatic molecules via  $\pi$ – $\pi$  interaction. Noncovalent functionalization can be used to tune the electronic properties of graphene without changing its aromatic character.

## 3. Covalent Functionalization Approaches

### 3.1. Amino Group

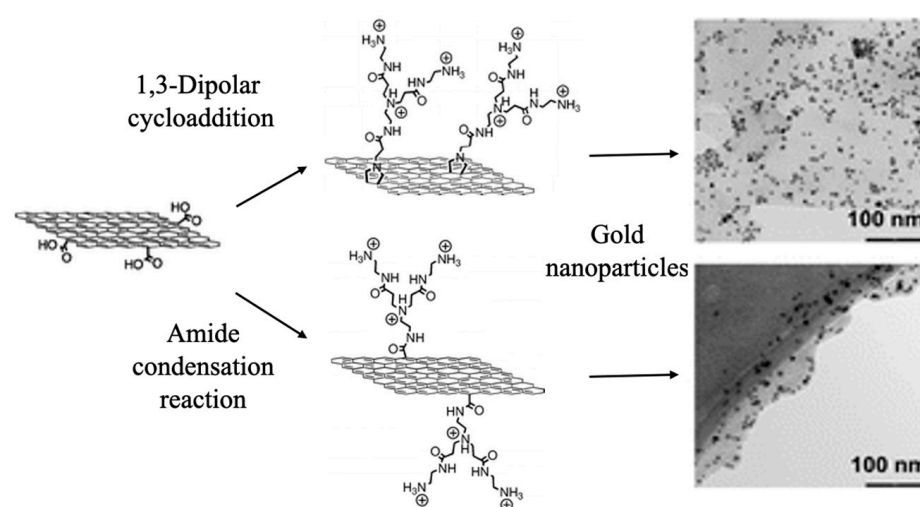
Prato et al. constructed the pyrrolidine ring via a 1,3-dipolar cycloaddition reaction between azomethine ylides and liquid-phase exfoliated graphene to introduce the amino groups (Scheme 2) [16]. The covalent functionalization was confirmed by the increase in  $I_D/I_G$  in the Raman spectra. The presence of carbon atoms with various binding energy in

the XPS clearly shows that the organic molecule was successfully combined with graphene. TGA analysis indicates the functionalization degree is one functional group in each of the 128 carbon atoms. Gold nanorods were used as an indicator to locate the sites of amino functionalization. TEM measurement demonstrated that the functionalization happened both on the edges and the basal plane of graphene.



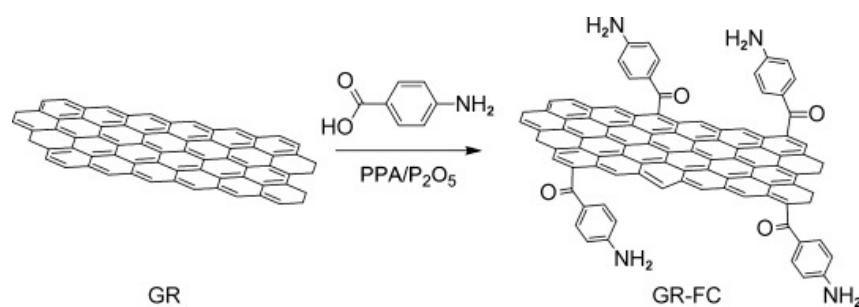
**Scheme 2.** 1,3-Dipolar cycloaddition functionalized graphene derivatives. Reproduced with permission from [16], copyright 2010 American Chemical Society.

Another study was also deployed by Prato and coworkers (Scheme 3) [17]. They compared the functionalization between 1,3-dipolar cycloaddition and an amide condensation reaction. XPS and Kaiser's test shows a higher extent of functionalization with a 1,3-dipolar cycloaddition reaction. After adding Au nanoparticles (NPs), TEM images show amide condensation mainly occurs at the edges of the pristine graphene while the former approach can happen both on the edge and the basal plane of GNPs.



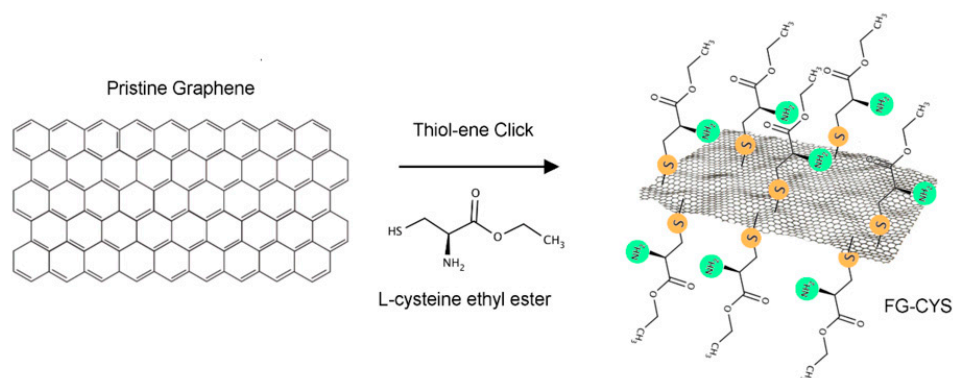
**Scheme 3.** Functionalization of graphene via 1,3-dipolar cycloaddition and amide condensation reaction. Reproduced with permission from [17], copyright 2011 The Royal Society of Chemistry.

Pumera et al. reported the covalent functionalization of GNPs via the Friedel–Crafts reaction under mild conditions of polyphosphoric acid/phosphorus pentoxide and 4-aminobenzoic acid (Scheme 4) [18]. The increase in the  $I_D/I_G$  ratio in the Raman spectra confirmed the covalent combination. The increase in intensity of the oxygen peak at 531.8 eV corresponds to the result of the acylation reaction. A shoulder peak at 288.9 eV and a new peak at 399.3 eV in the XPS correspond to the C=O bond and the nitrogen elements, respectively, indicating the success of the Friedel–Crafts acylation reaction. The overlap of the N-H stretching bands at 3460 and 3360  $\text{cm}^{-1}$  and the C=O stretching band at 1658  $\text{cm}^{-1}$  in the IR suggest the successful functionalization of graphene with 4-aminobenzoic acid.



**Scheme 4.** Functionalization of GNPs via the Friedel–Crafts reaction. Reproduced with permission from [18], copyright 2012 John Wiley & Sons.

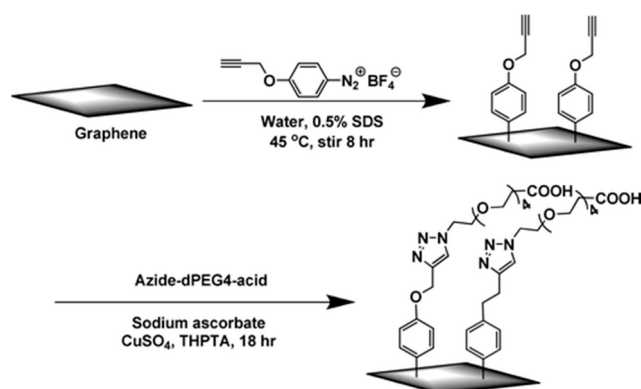
A thiol–ene click reaction between L-cysteine ethyl ester and graphene was deployed by Dusan’s group to introduce amino groups to pristine graphene (Scheme 5) [19]. The functionalized graphene shows a significant increase in the S2p, N1s, and O1s peaks at 164.0 eV, 401.5 eV, and 531.0 eV in the XPS spectra, indicating the presence of L-cysteine ethyl ester. A new vibration band between 600–800  $\text{cm}^{-1}$  in the IR spectrum for the functionalized graphene confirmed the formation of the C–S bond. The covalent interaction was corroborated with the increase in the  $I_D/I_G$  ratio from 0.3 to 0.7 in the Raman spectra. The density of the functional groups was estimated to be 1 cysteine molecule per 113 carbon atoms via the weight loss in the TGA. Remarkably, the amino functionalized graphene can be stably dispersed in water for one week due to the hydrogen bonding between the thiol precursor and water, in contrast the pristine graphene sedimented within two hours.



**Scheme 5.** The thiol–ene click reaction between L-cysteine ethyl ester and graphene. Reproduced with permission from [19], copyright 2021 Multidisciplinary Digital Publishing Institute.

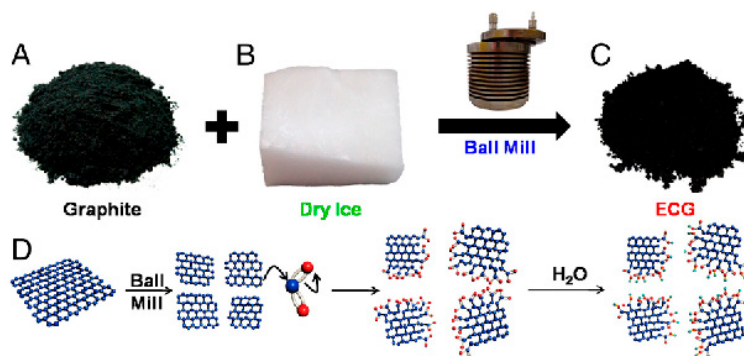
### 3.2. Carboxylic Acid Group

The functionalized GNPs can also be further modified via click chemistry. Strano et al. successfully functionalized solution-dispersed GNPs and CVD monolayer graphene using 4-propargyloxybenzenediazonium tetrafluoroborate and azido-dPEG4-acid, which provided a short-chain polyethylene glycol with a terminal carboxylic group (Scheme 6) [20]. The increase in saturated concentration of graphene in water was observed in the UV-Vis absorption spectrum. Surface tension and zeta-potential measurement indicate that the high degree of grafting density is an important factor in stabilizing the functionalized graphene in water. The increase in the  $I_D/I_G$  band ratio reveals the covalent functionalization, and the  $I_D/I_G$  spatial map indicates the functionalization prefers to occur on the edges.



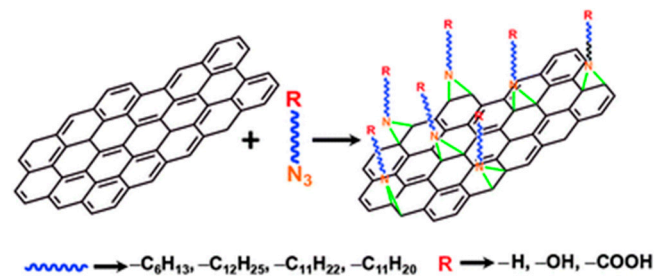
**Scheme 6.** Diazonium reaction on graphene and subsequent functionalization using click chemistry. Reproduced with permission from [20], copyright 2011 American Chemical Society.

A ball milling reaction is also widely used for the chemical functionalization of GNPs. Baek and Dai successfully introduced carboxyl group to the edge of GNPs via ball milling with dry ice (Scheme 7) [21]. SEM and TEM images show that the pristine graphite was directly exfoliated into single- and few-layer GNPs simply by ball milling with dry ice. Based on the oxygen content and the C/O ratio from element analysis, the functionalization degree was estimated as each 7.26 carbons possessing one carboxylic acid group. As expected, the unique peaks of the carboxyl group at  $1718\text{ cm}^{-1}$  can be observed in the IR spectrum. In the Raman spectra, the  $I_D/I_G$  ratio of the edges is much higher than the ratio of the basal plane, demonstrating that the functionalization occurred mainly on the edges of the GNPs. The intensity of oxygen peak in the XPS showed a significant increase, indicating the presence of oxygen-rich groups. Later, the ball milling method was also used by the same group to introduce sulfonic acid groups and carboxylic acid groups to the edge of GNPs [22]. Mülhaupt's group successfully increased the thermal conductivity of polymer nanocomposites by incorporation of carboxylated GNPs obtained from the ball milling method [23].



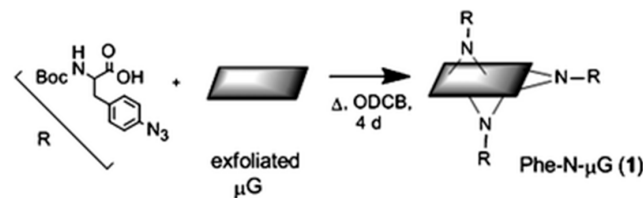
**Scheme 7.** (A) Pristine graphite; (B) dry ice (solid phase  $\text{CO}_2$ ); (C) edge-carboxylated graphite; (D) a schematic representation of the ball milling reaction. Reproduced with permission from [21], copyright 2012 United States National Academy of Sciences.

In another example, Valiyaveetil's group successfully introduced carboxyl groups with the use of 1-azidoundecanoic acid via an azide addition reaction by releasing free  $\text{N}_2$  (Scheme 8) [24]. The functionalized GNPs can be dispersed in common organic solvents, such as *N,N*-dimethylformamide (DMF), for a few days. With the combination of gold nanoparticles, the carboxylic group can be identified at the edges and the basal plane of the GNPs using TEM. The missing peaks of azides in the IR spectrum and the increase in the  $I_D/I_G$  band ratio in the Raman spectra indicate the successful covalent functionalization of GNPs.



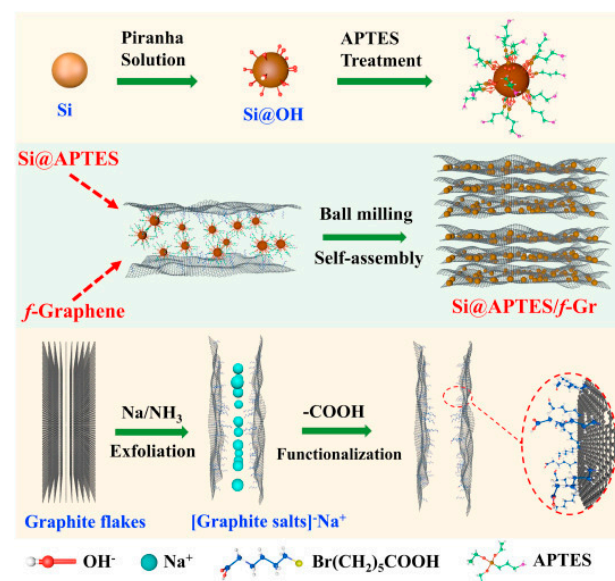
**Scheme 8.** Schematic representation of the covalent functionalization of GNPs with alkylazides. Reproduced with permission from [24], copyright 2011 The Royal Society of Chemistry.

Barron's group reported an azidophenylalanine functionalized GNPs via nitrene addition (Scheme 9) [25]. By using XPS and IR, the existence of alanine was confirmed. The degree of functionalization was determined to be 1 phenylalanine per 13 carbons via the TGA measurement. The increase in the  $I_D/I_G$  ratio in the Raman spectra indicates the covalent connection between phenylalanine and GNPs.



**Scheme 9.** Nitrene addition to exfoliated micro-crystalline graphite in refluxing *o*-dichlorobenzene (ODCB). Reproduced with permission from [25], copyright 2010 The Royal Society of Chemistry.

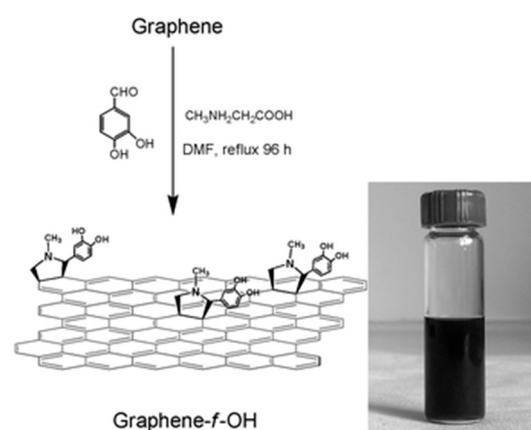
Wang and coworkers successfully introduced the carboxylic acid groups onto GNPs via a modified Birch reduction (Scheme 10) [26]. The functionalized GNPs can be further modified with Si nanoparticles. After functionalization, the  $I_D/I_G$  ratio has increased from 0.29 to 1.13, indicating the successful covalent connection. The peaks at 285.99 eV and 289.00 eV in the XPS corresponds to the C-O double bonds and the carboxylic acid groups, respectively. The O-H stretching at  $\sim 3007 \text{ cm}^{-1}$  and the carbonyl stretching at  $\sim 1820 \text{ cm}^{-1}$  demonstrate the successful functionalization of GNPs with carboxylic acid groups.



**Scheme 10.** The fabrication of Si@APTES/*f*-Gr composite. Reproduced with permission from [26], copyright 2021 Elsevier.

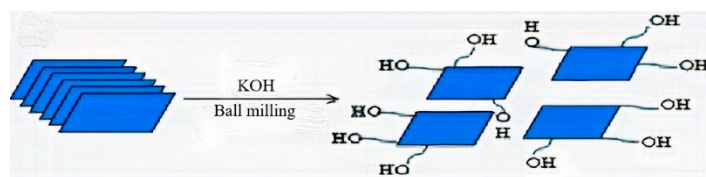
### 3.3. Hydroxyl Group

Georgakilas et al. used 1,3-dipolar cycloaddition of azomethine ylide to introduce the hydroxyl group to the dispersion of GNPs in pyridine (Scheme 11) [27]. The functionalized GNPs can be stably dispersed in ethanol for 30 days. The increase in the monolayer thickness from the AFM measurement reveals that the functional groups exist across the graphene surface. The increased  $I_D/I_G$  ratio in the Raman spectra indicates the covalent connection between the functional group and the GNPs. The 25% weight loss between 250 and 350 °C can be observed in the TGA measurement, which corresponds to the attached organic groups. The existence of the C–O stretching band at  $1250\text{ cm}^{-1}$  and the O–H stretching band at  $3500\text{ cm}^{-1}$  in the IR prove the presence of phenols.



**Scheme 11.** 1,3-dipolar cycloaddition of azomethine ylide on graphene and dispersion of graphene-*f*-OH in ethanol. Reproduced with permission from [27], copyright 2010 The Royal Society of Chemistry.

Hydroxyl-functionalized graphene was obtained by Dai's group via ball milling exfoliation of graphite with potassium hydroxide (Scheme 12) [28]. The hydroxyl-functionalized graphene is highly electroactive, hydrophilic, and water-dispersible. AFM images reveal that the functionalized graphene consists of single- to few-layer GNPs. The O–H stretching band at around  $3400\text{ cm}^{-1}$  in the IR spectrum indicates the hydroxyl group was introduced onto the graphene. The corresponding peak was also observed in the XPS spectrum.

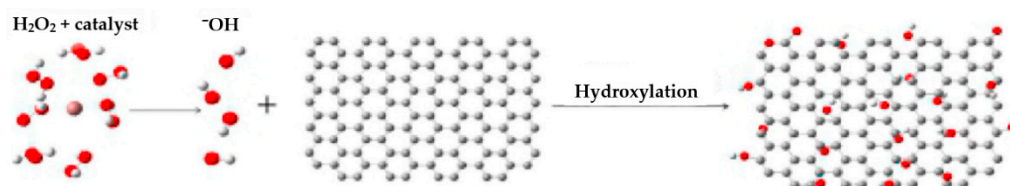


**Scheme 12.** Schematic of the synthesis of hydroxyl-functionalized graphene via ball milling. Reproduced with permission from [28], copyright 2012 The Royal Society of Chemistry.

Sun and coworkers successfully introduced poly(vinyl)alcohol to GNPs via esterification [29]. The carboxylic group on prefunctionalized GNPs was acquired by the oxidation of GNPs in a cold nitric/sulfuric acid mixture, combined with prolonged sonication. The functionalized GNPs can be easily dispersed in DMSO and hot water. The peak at  $1730\text{ cm}^{-1}$  in the IR spectrum hints the ester linkage between the polyvinyl alcohol (PVA) and the GNPs. TEM images show a similar thickness with the prefunctionalized GNPs, which indicates that the functionalization has no significant effects on the nanostructures of GNPs. The increase in the glass transition temperature  $T_g$  in the DSC measurement demonstrates that the linkage with GNPs decrease the polymer chain mobility substantially. The similar increase in the  $I_D/I_G$  ratio was also observed in the Raman spectra.

A microwave-assisted electrophilic reaction was deployed by Amiri et al. to functionalize GNPs with ethylene glycol [30]. The functionalized GNPs show a good dispersibility in water/ethylene glycol media. The broad peaks at 3486 and 1141  $\text{cm}^{-1}$  in the IR spectra correspond to the O-H and C-O stretching vibrations. The increased ratios of the D-G band ( $I_D/I_G$ ) can be seen when compared with the pristine GNPs, indicating that some  $\text{sp}^2$ -hybridized carbons changed to the  $\text{sp}^3$  hybridization. The steady weight loss between 140 and 500  $^\circ\text{C}$  in the TGA corresponds to the ethylene glycol group. However, the exact mechanism for the functionalization of GNPs is not clear discussed in the study.

In another report, Qin et al. successfully introduced the hydroxyl group to GNPs via the free radical reaction of hydrogen peroxide (Scheme 13) [31]. The peaks at 533.2, 532.0, and 530.2 eV in the XPS are attributed to the phenolic hydroxyl, aliphatic hydroxyl, and carbonyl groups, respectively. The functionalized graphene shows a much better dispersibility in water than the pristine graphene, mainly due to the introduction of the -OH groups. By adjusting the reaction time, the bandgap of the functionalized graphene can be tuned from 0.72 to 1.88 eV.



**Scheme 13.** The hydroxylation procedure of graphene. Reproduced with permission from [31], copyright 2021 Elsevier.

Covalent functionalization of GNPs can provide more stable connection between GNPs and functional units compared with the noncovalent approach. Covalent functionalization may significantly change the electronic properties of GNPs [32]. However, it is still a convenient way to obtain functionalized GNPs with hydroxyl, amino, and carboxylic terminal groups.

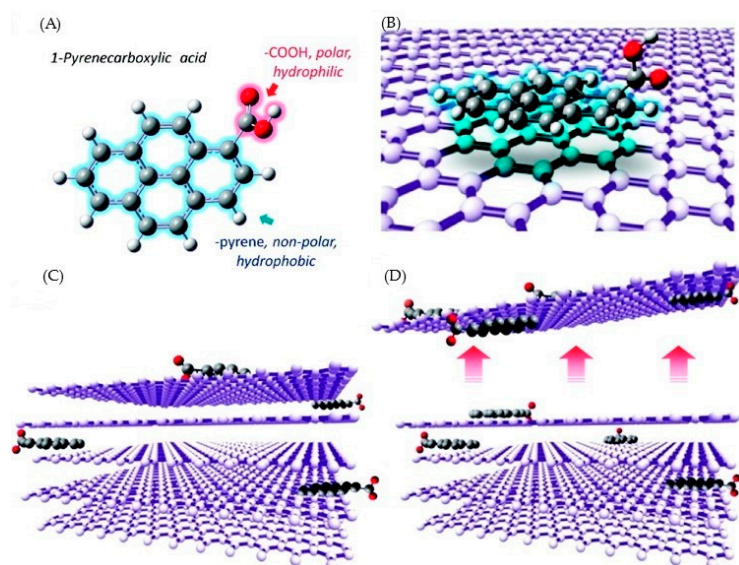
#### 4. Noncovalent Functionalization Approaches

##### 4.1. Hydroxyl Group

The dispersibility of GNPs can also be enhanced via noncovalent functionalization, as demonstrated by Horacio's group [33]. The PVA chain was covalently connected to *N*-(carboxyphenyl)-*N'*-(8-pentadecyl)perylene-3,4,9,10-bis(dicarboximide) and then combined with GNPs through  $\pi$ - $\pi$  interaction. The peak at 275 nm in the UV absorption spectrum indicates the existence of GNPs. The emission spectrum shows that GNPs have a significant quenching effect even in low concentrations. The second order 2D peak in the Raman spectrum offers a strong evidence that the lowest estimated thicknesses of the nanoplatelets are between 2 and 4 layers. The polymeric surfactant adjusts the membrane-forming ability to form stable and homogeneous solid films.

##### 4.2. Carboxylic Acid Group

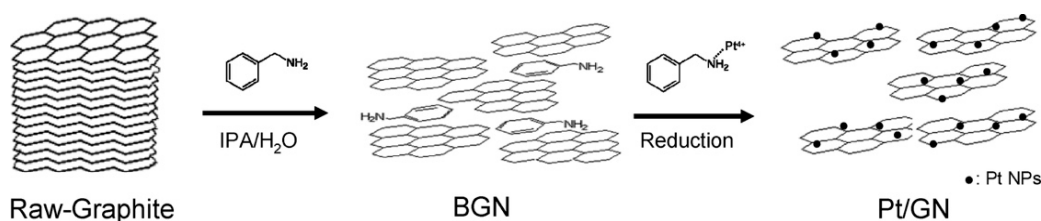
Kar et al. successfully dispersed GNPs in water by sonicating graphite in 1-pyrenecarboxylic acid solution (Scheme 14) [34]. The single Lorentzian shape of the second-order zone-boundary phonon peak in the Raman spectrum indicates the monolayer nature of graphene. The pyrenecarboxylic acid can cleave graphite layers and can also stabilize the dispersion of graphene sheets due to  $\pi$ - $\pi$  interaction. The functionalized GNPs can be used as a sensor to detect alcohols because of the rapid increase in the resistance.



**Scheme 14.** Noncovalent functionalization of GNPs with pyrenecarboxylic acid. (A) Molecular structure of 1-pyrenecarboxylic acid. (B) A PCA molecule can form a stable  $\pi$ -stacking interaction with graphene. (C) In a polar medium, pyrene prefers to attach itself on top of the graphene. With continuous agitation, more pyrenes enter in between the layers and move in deeper, breaking the  $\pi$ -bonding of the graphite. (D) Continuing this process releases single- and few-layer graphene. The hydrophilic -COOH groups of the PCA molecules prefer the polar medium and keep the graphene flakes stably dispersed in water. Reproduced with permission from [34], copyright 2010 American Chemical Society.

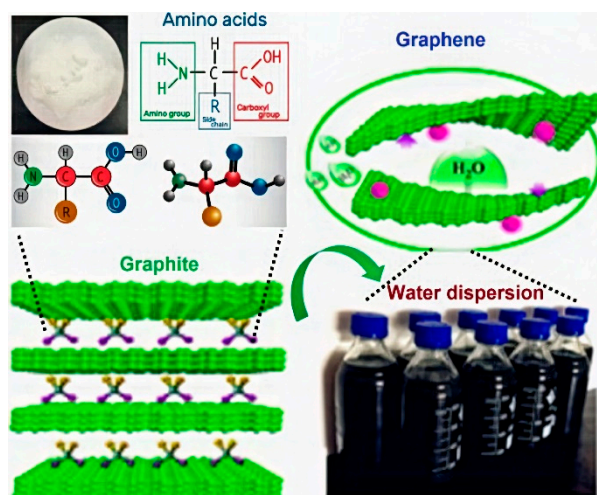
#### 4.3. Amino Group

Kuo et. al. reported the benzylamine-assisted noncovalent exfoliation of GNPs (Scheme 15) [35]. TEM images show that the sheet size of the exfoliated GNPs is between 100–300 nm. The increase in the ratios of the D/G band indicates that the ultrasonic condition introduces defects associated with new edges. Pt particles were connected to benzylamine as a stabilizer. The hybrids were used as electrodes, which showed an excellent catalytic ability toward methanol oxidation.



**Scheme 15.** The synthetic procedure of Pt/GNPs. Reproduced with permission from [35], copyright 2011 American Chemical Society.

Yu and co-workers used an amino acid-assisted ball-milling method for the exfoliation of graphene (Scheme 16) [36]. The exfoliated graphene can be dispersed in various polar solvents. The peaks between  $3200\text{--}3300\text{ cm}^{-1}$  in the IR spectra correspond to the O-H and N-H groups, respectively, which can prove the presence of amino acids. The TGA curve shows an obvious weight loss of 4.4% corresponding to the content of organic groups. Additionally, the peaks at 285.8 and 287.5 eV can be observed in the XPS spectrum, which can also prove the existence of the amino acids. A similar exfoliation of graphene with triazine was also reported by Vazquez and coworkers [37].



**Scheme 16.** The schematic presentation of amino acid assisted exfoliation of graphene. Reproduced with permission from [36], copyright 2018 American Chemical Society.

Noncovalent functionalization can tune the properties of GNPs by introducing functional groups without disturbing the electronic network. However, the force based on  $\pi$ - $\pi$  interaction, electrostatic interaction, and/or hydrophobic interaction is apparently weaker than the covalent connection. When further functionalization steps are needed, desorption of molecules from GNPs may happen, which can disturb the subsequent functionalization. Therefore, more care and stable measures should be taken when working with multistep noncovalent functionalization methods.

The different covalent and noncovalent functionalization approaches including materials, reagents, methods, terminal groups, and characterization techniques are summarized in Table 1.

**Table 1.** Covalent and noncovalent functionalization approaches of GNPs.

Ref.	Materials	Covalent Approaches			
		Reagents	Methods	Terminal Groups	Characterization Techniques
[16]	Liquid-phase exfoliated graphene	Azomethine ylides	1,3-dipolar cycloaddition	Amino group	Raman, XPS, TGA, TEM and UV
[17]	Exfoliated graphene in DMF	PAMAM Dendron	1,3-dipolar cycloaddition	Amino group	Kaiser's test, Raman, XPS, TGA, TEM, AFM and UV
[18]	Graphene nanosheet	4-amino-benzoic Acid	Friedel-Crafts acylation	Amino group	XPS, FTIR, and Raman
[19]	Graphene	L-cysteine ethyl ester	Thiol-ene click reaction	Amino group	SEM, TEM, XPS, Raman, FTIR, and TGA
[20]	Solution-dispersed and CVD graphene	4-propargyl-oxybenzenediazonium tetrafluoroborate and azido-dPEG4-acid	Diazonium reaction and 1,3-dipolar cycloaddition	Carboxylic acid group	XPS, FTIR, Raman, TEM, SEM, and TGA
[21]	Graphene nanoplatelets	Dry ice	Solid-state reaction	Carboxylic acid group	XPS, FTIR, Raman, TEM, SEM, and XRD
[24]	Graphene nanoplatelets	Various alkylazides	Nitrene addition	Carboxylic acid group	XPS, FTIR, Raman, TEM, SEM, STM, AFM, NMR and XRD
[25]	Exfoliated micro-crystalline graphene in ODCB	Azido-phenylalanine	Nitrene addition	Carboxylic acid group	XPS, FTIR, Raman, TEM, SEM, STM, AFM, and TGA
[26]	Graphene	Ammonia, 6-bromohexanoic acid	Birch reduction	Carboxylic acid group	Raman, XPS, FTIR, SEM, TEM, and EDS
[27]	Graphene in pyridine	Azomethine ylide	1,3-dipolar cycloaddition	Hydroxyl group	XPS, FTIR, Raman, TEM, SEM, AFM, and TGA
[28]	Graphite	Solid KOH	Solid-state reaction	Hydroxyl group	XPS, FTIR, Raman, TEM, SEM, STM, AFM, NMR and XRD
[29]	Graphene nanoplatelets	poly(vinyl)alcohol	Esterification	Hydroxyl group	XPS, FTIR, Raman, TEM, SEM, and NMR
[30]	Graphene nanoplatelets	Ethylene glycol	Electrophilic reaction	Hydroxyl group	FTIR, Raman, TEM, and TGA
[31]	Graphene	Hydrogen peroxide	Free radical reaction	Hydroxyl group	XPS, Raman, TEM, TGA, and UV

Table 1. Cont.

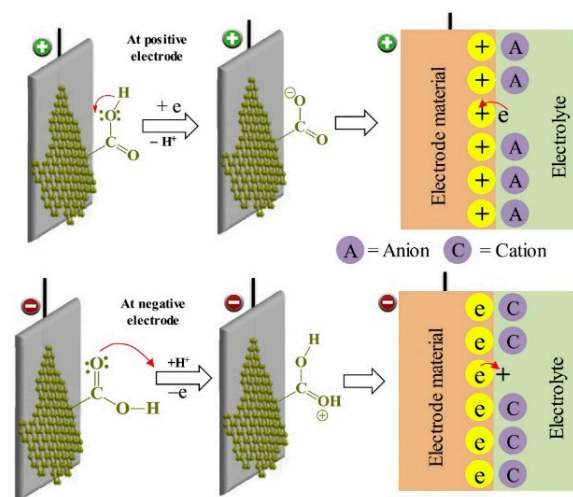
Noncovalent Approaches					
Ref.	Materials	Reagents	Methods	Terminal Groups	Characterization Techniques
[33]	Graphene	<i>N</i> -(carboxy-phenyl)- <i>N'</i> -(8-penta-decyl)perylene-3,4:9,10-bis(dicarboximide)	$\pi$ - $\pi$ interaction	Hydroxyl group	UV, Raman, DSC, and SEM
[34]	Graphene	Pyrenecar-boxylic acid	$\pi$ - $\pi$ interaction	Carboxylic acid group	TEM, SEM, AFM, Raman, UV-Vis
[35]	Physically exfoliated graphite nanoplatelets	Benzylamine	$\pi$ - $\pi$ interaction	Amino group	TEM, Raman, XRD
[36]	Graphite	Amino acid	$\pi$ - $\pi$ interaction	Amino group and carboxylic acid group	FTIR, TGA, XPS

PAMAM: poly(amidoamine).

## 5. Applications

Functionalized GNPs have already found applications in various fields, such as energy conversion and storage, nanocomposites, coatings, sensing, catalysts, and biological applications.

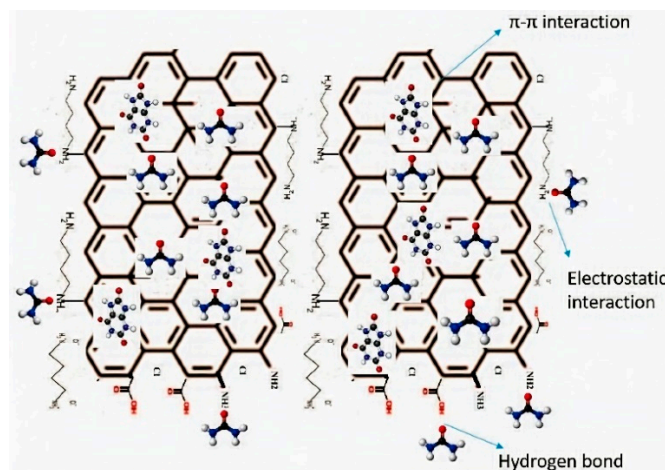
Supercapacitor is a kind of energy storage device between lithium-ion battery and traditional capacitor [38,39]. It has drawn a lot of interest due to the strong demand for lightweight, flexible, portable, and high-performance energy storage devices. Owing to the large specific surface area, high conductivity, and stability, graphene and its derivatives can be considered as candidates for electrode materials [6,40]. The introduction of heteroatoms can increase the specific capacitance of supercapacitors. Several studies have reported that carboxylic graphene can be used as the electrode materials for supercapacitors [41–45]. Baek et al. have successfully introduced carboxylic groups to GNPs via a ball milling reaction [46]. The existence of the carboxylic groups is able to increase the electroactive surface area and wettability of GNPs, and also enables ion adsorption and rapid electrolyte diffusion. In the meanwhile, reversible pseudo-capacitive reactions can also occur on the carboxylic groups (Scheme 17). The specific capacitance ( $C_{sp}$ ) of the edge functionalized graphene can reach  $365.72 \text{ F g}^{-1}$  at a current density of  $1 \text{ A g}^{-1}$ , demonstrating the potential applications for high-performance energy storage devices.



**Scheme 17.** Proposed mechanism for the reversible pseudo-capacitive reactions of edge functionalized graphene. Reproduced with permission from [46], copyright 2018 Elsevier.

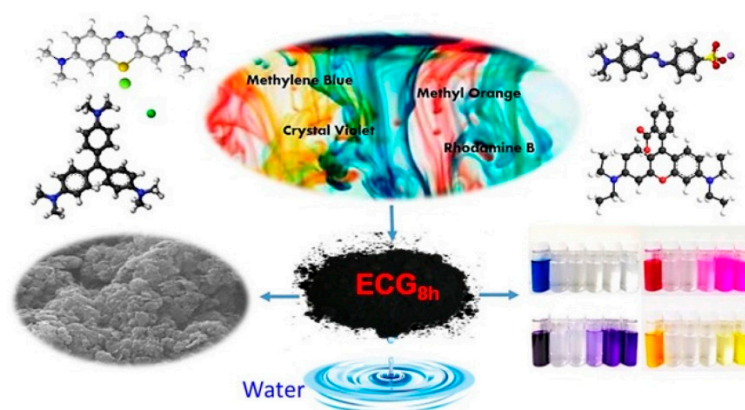
Chronic kidney disease (CKD) is a worldwide public health problem. In stage III and stage IV of this disease, the toxic urea or uric acid can only be removed by absorption, which is called hemodialysis. Using carbon-based materials is one of the most promising approaches towards this direction due to their high adsorption capacity [47,48], excellent hemocompatibility and relatively low cost. These materials have been demonstrated in

adsorbing different kinds of compounds and heavy metal ions [49–51]. Cabello-Alvarado et al. developed amino modified GNPs as a potential absorbent (Scheme 18) [52]. Using the functionalized GNPs, the maximum percentage of absorption of uremic toxins was 97%. It is worth mentioning that, at the concentration of 500 mg/mL, the functionalized GNPs show no cytotoxicity and extremely low degree of hemolysis (<2%).



**Scheme 18.** The mechanism of urea and uric acid adsorption onto the modified GNPs. Reproduced with permission from [52], copyright 2019 Multidisciplinary Digital Publishing Institute.

Removing different charged dyes from industrial effluent water is very important to society for solving pollution problems and obtaining clean water. Functionalized GNPs can also be used to remove industrial dyes from effluent water. Hung and coworkers reported edge-functionalized GNPs as absorbents for the removal of oppositely charged dye ions (Scheme 19) [53]. The carboxylic acid group was introduced to the edge of GNPs via a dry ball milling reaction. The 8-h ball-milling product shows a high surface area of  $387.69 \text{ m}^2 \text{ g}^{-1}$  and a total pore volume of  $0.55 \text{ cm}^3 \text{ g}^{-1}$ . The functionalized graphene can absorb  $99.32 \pm 0.2\%$  of the differently charged dye ions within 5–20 min, demonstrating its high potential for water purification.



**Scheme 19.** The edge-carboxylate GNPs absorbent for different dye ions. Reproduced with permission from [53], copyright 2020 Elsevier.

Epoxy resin is a kind of lightweight thermoset material that has been widely used in high-performance composites. The advantages of epoxy include, but are not limited to, low cost, durability under different temperatures, anti-corrosive nature, and high weight to strength ratio [54,55]. However, the low thermal conductivity and a high coefficient of friction have limited the applications of epoxy resin [56]. GNPs are expected to provide a better reinforcing effect in polymer composites with greatly improved mechanical and

thermal properties. Hossain et al. deployed amino-functionalized GNPs as a nanofiller to reinforce the epoxy resin [57]. The 0.4 wt% GNPs modified carbon fiber/epoxy composites exhibited the best properties, with a 19% increase in the flexure strength and a 15% improvement in the flexure modulus. The composite also showed an 18% and 19% increase in the tensile strength and the tensile modulus, respectively.

Metal corrosion problems have been associated with the history of human beings using metal, and countless attempts have been made to improve the corrosion resistance of metals. Due to higher corrosion resistance and outstanding adhesion, epoxy coating has drawn much attention among different methods [58,59]. Zhao's group has successfully used poly(2-butylaniline) functionalized graphene as an additive in epoxy coating [60]. A remarkable improvement on anti-corrosion performance can be observed with the addition of 0.5–1 wt% functionalized GNPs to the epoxy matrix. Moreover, the composite shows an improvement in the reduction in the friction coefficient and the wear resistance under dry conditions.

Besides the above discussed examples, functionalized GNPs using noncovalent methods have also been used for different applications. For example, with the noncovalently functionalized GNPs, Kar et al. developed a highly selective and sensitive conductometric sensors, which can show a rapid change in its resistance (>10,000%) when exposing to saturated ethanol vapors [34]. A supercapacitor with a high specific capacitance (~120 F/g), good power density (~105 kW/kg), and energy density (~9.2 Wh/kg) was also reported in the same study. One year later, Kuo et al. deposited Pt nanoparticles onto the amino-functionalized GNPs, and the composite showed an excellent catalytic ability towards methanol oxidation [35]. A 60% increment in mass activity was realized with the Pt/GN composite compared with that of commercial Pt/XC-72.

## 6. Conclusions and Outlook

The functionalization of GNPs has been well developed in recent years. Amino, hydroxyl, and carboxylic acid groups can be introduced onto GNPs using both covalent and noncovalent methods. With these groups, dispersibility of GNPs in solvents can be significantly improved. Furthermore, these terminal groups can be employed as linkers for further functionalization.

Covalent functionalization of GNPs can change the electronic properties of GNPs since the degree of functionalization is tightly related to the properties. On the other hand, more methods of covalent functionalization of GNPs should also be developed to broaden the chemistry of GNPs and to meet the needs of practical applications. Compared with covalent functionalization, the connection of noncovalent functionalization between GNPs matrix and functional groups is weaker. The advantage of noncovalent functionalization is also significant. Noncovalent functionalization can introduce functional groups without disturbing the electronic network of GNPs to a considerable extent [61], and noncovalent functionalization can be deployed under a mild condition through electrostatic interaction, hydrophobic interaction, and  $\pi$ - $\pi$  interaction. Preparation of functionalized GNPs in bulk quantities with high dispersibility and long-term stability in different solvents is currently in high demand.

As one of the most developed 2D materials, the preparation and functionalization of GNPs still suffer from the limited methods. It is inevitable to solve these synthetic problems so that GNPs can be attached with novel functional molecules to obtain functionalized GNPs with hydroxyl, amino, and carboxylic terminal groups under milder and environmentally friendly conditions such as lower temperature, shorter reaction time, aerobic atmosphere, and aqueous media. With newly developed methods, novel functionalized GNPs derivatives with specific terminal groups can be prepared and be further employed in different applications such as supercapacitors [62–64], fuel cells [65], drug delivery [66], nanocomposites, controllable massive transport [67], and many other areas [68–72].

**Author Contributions:** Conceptualization, X.Z.; writing and editing, C.P. and X.Z. All authors have read and agreed to the published version of the manuscript.

**Funding:** The authors would like to thank the financial support from 2D TECH VINNOVA competence Center (Ref. 2019-00068) and Stiftelsen Chalmers tekniska högskola.

**Data Availability Statement:** All data used in this article are publicly available.

**Conflicts of Interest:** The authors declare no conflict of interest.

## References

1. Novoselov, K.S.; Geim, A.K.; Morozov, S.V.; Jiang, D.; Zhang, Y.; Dubonos, S.V.; Grigorieva, I.V.; Firsov, A.A. Electric field effect in atomically thin carbon films. *Science* **2004**, *306*, 666–669. [[CrossRef](#)]
2. Reina, A.; Jia, X.; Ho, J.; Nezich, D.; Son, H.; Bulovic, V.; Dresselhaus, M.S.; Kong, J. Large area, few-layer graphene films on arbitrary substrates by chemical vapor deposition. *Nano Lett.* **2009**, *9*, 30–35. [[CrossRef](#)]
3. Huh, S.; Park, J.; Kim, K.S.; Hong, B.H.; Kim, S.B. Selective n-type doping of graphene by photo-patterned gold nanoparticles. *ACS Nano* **2011**, *5*, 3639–3644. [[CrossRef](#)]
4. Wang, Y.; Li, Z.; Wang, J.; Li, J.; Lin, Y. Graphene and graphene oxide: Biofunctionalization and applications in biotechnology. *Trends Biotechnol.* **2011**, *29*, 205–212. [[CrossRef](#)] [[PubMed](#)]
5. Geim, A.K. Graphene: Status and prospects. *Science* **2009**, *324*, 1530–1534. [[CrossRef](#)]
6. Novoselov, K.S.; Fal'ko, V.I.; Colombo, L.; Gellert, P.R.; Schwab, M.G.; Kim, K. A roadmap for graphene. *Nature* **2012**, *490*, 192–200. [[CrossRef](#)] [[PubMed](#)]
7. Ferrari, A.C.; Bonaccorso, F.; Fal'ko, V.; Novoselov, K.S.; Roche, S.; Bøggild, P.; Borini, S.; Koppens, F.H.L.; Palermo, V.; Pugno, N.; et al. Science and technology roadmap for graphene, related two-dimensional crystals, and hybrid systems. *Nanoscale* **2015**, *7*, 4598–4810. [[CrossRef](#)] [[PubMed](#)]
8. Lotya, M.; Hernandez, Y.; King, P.J.; Smith, R.J.; Nicolosi, V.; Karlsson, L.S.; Blighe, F.M.; De, S.; Wang, Z.; McGovern, I.T.; et al. Liquid phase production of graphene by exfoliation of graphite in surfactant/water solutions. *J. Am. Chem. Soc.* **2009**, *131*, 3611–3620. [[CrossRef](#)] [[PubMed](#)]
9. Kim, K.S.; Zhao, Y.; Jang, H.; Lee, S.Y.; Kim, J.M.; Kim, K.S.; Ahn, J.-H.; Kim, P.; Choi, J.-Y.; Hong, B.H. Large-scale pattern growth of graphene films for stretchable transparent electrodes. *Nature* **2009**, *457*, 706–710. [[CrossRef](#)] [[PubMed](#)]
10. Li, X.; Cai, W.; An, J.; Kim, S.; Nah, J.; Yang, D.; Piner, R.; Velamakanni, A.; Jung, I.; Tutuc, E.; et al. Large-area synthesis of high-quality and uniform graphene films on copper foils. *Science* **2009**, *324*, 1312–1314. [[CrossRef](#)]
11. Park, S.; Ruoff, R.S. Chemical methods for the production of graphenes. *Nat. Nanotechnol.* **2009**, *4*, 217–224. [[CrossRef](#)]
12. Shao, Y.; Wang, J.; Engelhard, M.; Wang, C.; Lin, Y. Facile and controllable electrochemical reduction of graphene oxide and its applications. *J. Mater. Chem.* **2010**, *20*, 743–748. [[CrossRef](#)]
13. Niyogi, S.; Bekyarova, E.; Itkis, M.E.; Zhang, H.; Shepperd, K.; Hicks, J.; Sprinkle, M.; Berger, C.; Lau, C.N.; deHeer, W.A.; et al. Spectroscopy of covalently functionalized graphene. *Nano Lett.* **2010**, *10*, 4061–4066. [[CrossRef](#)]
14. Zhang, X.; Hou, L.; Samori, P. Coupling carbon nanomaterials with photochromic molecules for the generation of optically responsive materials. *Nat. Commun.* **2016**, *7*, 11118. [[CrossRef](#)]
15. Zhang, X.; Huisman, E.H.; Gurram, M.; Browne, W.R.; van Wees, B.J.; Feringa, B.L. Supramolecular chemistry on graphene field-effect transistors. *Small* **2014**, *10*, 1735–1740. [[CrossRef](#)]
16. Quintana, M.; Spyrou, K.; Grzelczak, M.; Browne, W.R.; Rudolf, P.; Prato, M. Functionalization of graphene via 1,3-dipolar cycloaddition. *ACS Nano* **2010**, *4*, 3527–3533. [[CrossRef](#)]
17. Quintana, M.; Montellano, A.; del Rio Castillo, A.E.; Tendeloo, G.V.; Bittencourt, C.; Prato, M. Selective organic functionalization of graphene bulk or graphene edges. *Chem. Commun.* **2011**, *47*, 9330–9332. [[CrossRef](#)] [[PubMed](#)]
18. Chua, C.K.; Pumera, M. Friedel–Crafts acylation on graphene. *Chem. Asian J.* **2012**, *7*, 1009–1012. [[CrossRef](#)] [[PubMed](#)]
19. Farivar, F.; Lay Yap, P.; Tung, T.T.; Losic, D. Highly water dispersible functionalized graphene by thermal thiol-ene click chemistry. *Materials* **2021**, *14*, 2830. [[CrossRef](#)]
20. Jin, Z.; McNicholas, T.P.; Shih, C.-J.; Wang, Q.H.; Paulus, G.L.C.; Hilmer, A.J.; Shimizu, S.; Strano, M.S. Click chemistry on solution-dispersed graphene and monolayer CVD graphene. *Chem. Mater.* **2011**, *23*, 3362–3370. [[CrossRef](#)]
21. Jeon, I.-Y.; Shin, Y.-R.; Sohn, G.-J.; Choi, H.-J.; Bae, S.-Y.; Mahmood, J.; Jung, S.-M.; Seo, J.-M.; Kim, M.-J.; Wook Chang, D.; et al. Edge-carboxylated graphene nanosheets via ball milling. *Proc. Natl. Acad. Sci. USA* **2012**, *109*, 5588–5593. [[CrossRef](#)]
22. Jeon, I.-Y.; Choi, H.-J.; Jung, S.-M.; Seo, J.-M.; Kim, M.-J.; Dai, L.; Baek, J.-B. Large-scale production of edge-selectively functionalized graphene nanoplatelets via ball milling and their use as metal-free electrocatalysts for oxygen reduction reaction. *J. Am. Chem. Soc.* **2013**, *135*, 1386–1393. [[CrossRef](#)]
23. Burk, L.; Gliem, M.; Lais, F.; Nutz, F.; Retsch, M.; Mülhaupt, R. Mechanochemically carboxylated multilayer graphene for carbon/ABS composites with improved thermal conductivity. *Polymers* **2018**, *10*, 1088. [[CrossRef](#)]
24. Vadukumpully, S.; Gupta, J.; Zhang, Y.; Xu, G.Q.; Valiyaveetil, S. Functionalization of surfactant wrapped graphene nanosheets with alkylazides for enhanced dispersibility. *Nanoscale* **2011**, *3*, 303–308. [[CrossRef](#)] [[PubMed](#)]
25. Strom, T.A.; Dillon, E.P.; Hamilton, C.E.; Barron, A.R. Nitrene addition to exfoliated graphene: A one-step route to highly functionalized graphene. *Chem. Commun.* **2010**, *46*, 4097–4099. [[CrossRef](#)] [[PubMed](#)]
26. Zhang, Y.; Cheng, Y.; Song, J.; Zhang, Y.; Shi, Q.; Wang, J.; Tian, F.; Yuan, S.; Su, Z.; Zhou, C.; et al. Functionalization-assisted ball milling towards Si/graphene anodes in high performance Li-ion batteries. *Carbon* **2021**, *181*, 300–309. [[CrossRef](#)]

27. Georgakilas, V.; Bourlinos, A.B.; Zboril, R.; Steriotis, T.A.; Dallas, P.; Stubos, A.K.; Trapalis, C. Organic functionalisation of graphenes. *Chem. Commun.* **2010**, *46*, 1766–1768. [[CrossRef](#)] [[PubMed](#)]
28. Yan, L.; Lin, M.; Zeng, C.; Chen, Z.; Zhang, S.; Zhao, X.; Wu, A.; Wang, Y.; Dai, L.; Qu, J.; et al. Electroactive and biocompatible hydroxyl- functionalized graphene by ball milling. *J. Mater. Chem.* **2012**, *22*, 8367–8371. [[CrossRef](#)]
29. Veca, L.M.; Lu, F.; Meziani, M.J.; Cao, L.; Zhang, P.; Qi, G.; Qu, L.; Shrestha, M.; Sun, Y.-P. Polymer functionalization and solubilization of carbon nanosheets. *Chem. Commun.* **2009**, 2565–2567. [[CrossRef](#)]
30. Amiri, A.; Sadri, R.; Shanbedi, M.; Ahmadi, G.; Kazi, S.N.; Chew, B.T.; Zubir, M.N.M. Synthesis of ethylene glycol-treated Graphene Nanoplatelets with one-pot, microwave-assisted functionalization for use as a high performance engine coolant. *Energy Convers. Manag.* **2015**, *101*, 767–777. [[CrossRef](#)]
31. Qin, C.; Deng, H.; Ao, S.; Dai, Z.; Huang, J.; Ni, H.; Ye, P. High-quality graphene derivative: Hydroxylated graphene prepared by modification of aromatic ring. *Carbon* **2021**, *176*, 290–295. [[CrossRef](#)]
32. Loh, K.P.; Bao, Q.; Ang, P.K.; Yang, J. The chemistry of graphene. *J. Mater. Chem.* **2010**, *20*, 2277–2289. [[CrossRef](#)]
33. Salavagione, H.J.; Ellis, G.; Segura, J.L.; Gómez, R.; Morales, G.M.; Martínez, G. Flexible film materials from conjugated dye-modified polymer surfactant-induced aqueous graphene dispersions. *J. Mater. Chem.* **2011**, *21*, 16129–16135. [[CrossRef](#)]
34. An, X.; Simmons, T.; Shah, R.; Wolfe, C.; Lewis, K.M.; Washington, M.; Nayak, S.K.; Talapatra, S.; Kar, S. Stable aqueous dispersions of noncovalently functionalized graphene from graphite and their multifunctional high-performance applications. *Nano Lett.* **2010**, *10*, 4295–4301. [[CrossRef](#)] [[PubMed](#)]
35. Hsu, C.-H.; Liao, H.-Y.; Wu, Y.-F.; Kuo, P.-L. Benzylamine-assisted noncovalent exfoliation of graphite-protecting Pt nanoparticles applied as catalyst for methanol oxidation. *ACS Appl. Mater. Interfaces* **2011**, *3*, 2169–2172. [[CrossRef](#)] [[PubMed](#)]
36. Zhao, H.; Xu, B.; Ding, J.; Wang, Z.; Yu, H. Natural amino acids: High-efficiency intercalants for graphene exfoliation. *ACS Sustain. Chem. Eng.* **2019**, *7*, 18819–18825. [[CrossRef](#)]
37. León, V.; Rodriguez, A.M.; Prieto, P.; Prato, M.; Vázquez, E. Exfoliation of graphite with triazine derivatives under ball-milling conditions: Preparation of few-layer graphene via selective noncovalent interactions. *ACS Nano* **2014**, *8*, 563–571. [[CrossRef](#)]
38. Liu, Y.; Deng, R.; Wang, Z.; Liu, H. Carboxyl-functionalized graphene oxide–polyaniline composite as a promising supercapacitor material. *J. Mater. Chem.* **2012**, *22*, 13619–13624. [[CrossRef](#)]
39. Simon, P.; Gogotsi, Y. Materials for electrochemical capacitors. *Nat. Mater.* **2008**, *7*, 845–854. [[CrossRef](#)]
40. Hu, H.; Zhao, Z.; Zhang, R.; Bin, Y.; Qiu, J. Polymer casting of ultralight graphene aerogels for the production of conductive nanocomposites with low filling content. *J. Mater. Chem. A* **2014**, *2*, 3756–3760. [[CrossRef](#)]
41. Raymundo-Piñero, E.; Leroux, F.; Béguin, F. A high-performance carbon for supercapacitors obtained by carbonization of a seaweed biopolymer. *Adv. Mater.* **2006**, *18*, 1877–1882. [[CrossRef](#)]
42. Wang, H.; Hao, Q.; Yang, X.; Lu, L.; Wang, X. Graphene oxide doped polyaniline for supercapacitors. *Electrochem. Commun.* **2009**, *11*, 1158–1161. [[CrossRef](#)]
43. Kumar, N.A.; Choi, H.-J.; Shin, Y.R.; Chang, D.W.; Dai, L.; Baek, J.-B. Polyaniline-grafted reduced graphene oxide for efficient electrochemical supercapacitors. *ACS Nano* **2012**, *6*, 1715–1723. [[CrossRef](#)] [[PubMed](#)]
44. Wang, M.; Duong, L.D.; Mai, N.T.; Kim, S.; Kim, Y.; Seo, H.; Kim, Y.C.; Jang, W.; Lee, Y.; Suhr, J.; et al. All-solid-state reduced graphene oxide supercapacitor with large volumetric capacitance and ultralong stability prepared by electrophoretic deposition method. *ACS Appl. Mater. Interfaces* **2015**, *7*, 1348–1354. [[CrossRef](#)]
45. Xie, B.; Chen, Y.; Yu, M.; Shen, X.; Lei, H.; Xie, T.; Zhang, Y.; Wu, Y. Carboxyl-assisted synthesis of nitrogen-doped graphene sheets for supercapacitor applications. *Nanoscale Res. Lett.* **2015**, *10*, 332. [[CrossRef](#)]
46. Deb Nath, N.C.; Jeon, I.-Y.; Ju, M.J.; Ansari, S.A.; Baek, J.-B.; Lee, J.-J. Edge-carboxylated graphene nanoplatelets as efficient electrode materials for electrochemical supercapacitors. *Carbon* **2019**, *142*, 89–98. [[CrossRef](#)]
47. Irfan, M.; Irfan, M.; Idris, A.; Baig, N.; Saleh, T.A.; Nasiri, R.; Iqbal, Y.; Muhammad, N.; Rehman, F.; Khalid, H. Fabrication and performance evaluation of blood compatible hemodialysis membrane using carboxylic multiwall carbon nanotubes and low molecular weight polyvinylpyrrolidone based nanocomposites. *J. Biomed. Mater. Res. Part A* **2019**, *107*, 513–525. [[CrossRef](#)]
48. Andrade-Guel, M.; Cabello-Alvarado, C.; Cruz-Delgado, V.J.; Bartolo-Perez, P.; De León-Martínez, P.A.; Sáenz-Galindo, A.; Cadenas-Pliego, G.; Ávila-Orta, C.A. Surface modification of graphene nanoplatelets by organic acids and ultrasonic radiation for enhance uremic toxins adsorption. *Materials* **2019**, *12*, 715. [[CrossRef](#)] [[PubMed](#)]
49. Achazhiyath Edathil, A.; Hisham Zain, J.; Abu Haija, M.; Banat, F. Scalable synthesis of an environmentally benign graphene–sand based organic–inorganic hybrid for sulfide removal from aqueous solution: An insight into the mechanism. *New J. Chem.* **2019**, *43*, 3500–3512. [[CrossRef](#)]
50. Yuan, K.; Li, Y.; Huang, X.; Liang, Y.; Liu, Q.; Jiang, G. Templated synthesis of a bifunctional Janus graphene for enhanced enrichment of both organic and inorganic targets. *Chem. Commun.* **2019**, *55*, 4957–4960. [[CrossRef](#)]
51. Zhao, L.; Yang, S.-T.; Yilihamu, A.; Wu, D. Advances in the applications of graphene adsorbents: From water treatment to soil remediation. *Rev. Inorg. Chem.* **2019**, *39*, 47–76. [[CrossRef](#)]
52. Cabello-Alvarado, C.; Andrade-Guel, M.; Pérez-Alvarez, M.; Cadenas-Pliego, G.; Cortés-Hernández, D.A.; Bartolo-Pérez, P.; Ávila-Orta, C.A.; Cruz-Delgado, V.J.; Zepeda-Pedreguera, A. Graphene nanoplatelets modified with amino-groups by ultrasonic radiation of variable frequency for potential adsorption of uremic toxins. *Nanomaterials* **2019**, *9*, 1261. [[CrossRef](#)] [[PubMed](#)]
53. Sivakumar, M.; Yadav, S.; Hung, W.-S.; Lai, J.-Y. One-pot eco-friendly synthesis of edge-carboxylate graphene via dry ball milling for enhanced removal of acid and basic dyes from single or mixed aqueous solution. *J. Clean. Prod.* **2020**, *263*, 121498. [[CrossRef](#)]

54. Li, Y.; Wang, S.; He, E.; Wang, Q. The effect of sliding velocity on the tribological properties of polymer/carbon nanotube composites. *Carbon* **2016**, *106*, 106–109. [[CrossRef](#)]
55. Friedrich, K. Polymer composites for tribological applications. *Adv. Ind. Eng. Polym. Res.* **2018**, *1*, 3–39. [[CrossRef](#)]
56. Wang, F.; Drzal, L.T.; Qin, Y.; Huang, Z. Mechanical properties and thermal conductivity of graphene nanoplatelet/epoxy composites. *J. Mater. Sci.* **2015**, *50*, 1082–1093. [[CrossRef](#)]
57. Hossain, M.K.; Chowdhury, M.M.R.; Bolden, N.W. Optimized mechanical performance of carbon fiber-epoxy composite using amino-functionalized graphene nanoplatelets. In Proceedings of the ASME 2015 International Mechanical Engineering Congress and Exposition, Houston, TX, USA, 13–19 November 2015.
58. Xavier, J.R. Investigation on the anticorrosion, adhesion and mechanical performance of epoxy nanocomposite coatings containing epoxy-silane treated nano-MoO<sub>3</sub> on mild steel. *J. Adhes. Sci. Technol.* **2020**, *34*, 115–134. [[CrossRef](#)]
59. Ibrahim, M.; Kannan, K.; Parangusan, H.; Eldeib, S.; Shehata, O.; Ismail, M.; Zarandah, R.; Sadasivuni, K.K. Enhanced corrosion protection of epoxy/ZnO-NiO nanocomposite coatings on steel. *Coatings* **2020**, *10*, 783. [[CrossRef](#)]
60. Chen, C.; Qiu, S.; Cui, M.; Qin, S.; Yan, G.; Zhao, H.; Wang, L.; Xue, Q. Achieving high performance corrosion and wear resistant epoxy coatings via incorporation of noncovalent functionalized graphene. *Carbon* **2017**, *114*, 356–366. [[CrossRef](#)]
61. Karousis, N.; Tagmatarchis, N.; Tasis, D. Current progress on the chemical modification of carbon nanotubes. *Chem. Rev.* **2010**, *110*, 5366–5397. [[CrossRef](#)]
62. Choi, B.G.; Yang, M.; Hong, W.H.; Choi, J.W.; Huh, Y.S. 3D macroporous graphene frameworks for supercapacitors with high energy and power densities. *ACS Nano* **2012**, *6*, 4020–4028. [[CrossRef](#)]
63. Chen, C.-M.; Zhang, Q.; Huang, C.-H.; Zhao, X.-C.; Zhang, B.-S.; Kong, Q.-Q.; Wang, M.-Z.; Yang, Y.-G.; Cai, R.; Sheng Su, D. Macroporous ‘bubble’ graphene film via template-directed ordered-assembly for high rate supercapacitors. *Chem. Commun.* **2012**, *48*, 7149–7151. [[CrossRef](#)]
64. Zhu, Y.; Murali, S.; Stoller, M.D.; Ganesh, K.J.; Cai, W.; Ferreira, P.J.; Pirkle, A.; Wallace, R.M.; Cychosz, K.A.; Thommes, M.; et al. Carbon-based supercapacitors produced by activation of graphene. *Science* **2011**, *332*, 1537–1541. [[CrossRef](#)]
65. Yong, Y.-C.; Dong, X.-C.; Chan-Park, M.B.; Song, H.; Chen, P. Macroporous and monolithic anode based on polyaniline hybridized three-dimensional graphene for high-performance microbial fuel cells. *ACS Nano* **2012**, *6*, 2394–2400. [[CrossRef](#)] [[PubMed](#)]
66. Li, X.; Huang, X.; Liu, D.; Wang, X.; Song, S.; Zhou, L.; Zhang, H. Synthesis of 3D hierarchical Fe<sub>3</sub>O<sub>4</sub>/graphene composites with high lithium storage capacity and for controlled drug delivery. *J. Phys. Chem. C* **2011**, *115*, 21567–21573. [[CrossRef](#)]
67. Zhao, Y.; Xie, Y.; Liu, Z.; Wang, X.; Chai, Y.; Yan, F. Two-dimensional material membranes: An emerging platform for controllable mass transport applications. *Small* **2014**, *10*, 4521–4542. [[CrossRef](#)]
68. Maio, A.; Pibiri, I.; Morreale, M.; Mantia, F.P.L.; Scaffaro, R. An overview of functionalized graphene nanomaterials for advanced applications. *Nanomaterials* **2021**, *11*, 1717. [[CrossRef](#)]
69. Zhang, J.; Chen, G.; Müllen, K.; Feng, X. Carbon-rich nanomaterials: Fascinating hydrogen and oxygen electrocatalysts. *Adv. Mater.* **2018**, *30*, 1800528. [[CrossRef](#)]
70. Stergiou, A.; Cantón-Vitoria, R.; Psarrou, M.N.; Economopoulos, S.P.; Tagmatarchis, N. Functionalized graphene and targeted applications—Highlighting the road from chemistry to applications. *Prog. Mater. Sci.* **2020**, *114*, 100683. [[CrossRef](#)]
71. Huang, H.; Shi, H.; Das, P.; Qin, J.; Li, Y.; Wang, X.; Su, F.; Wen, P.; Li, S.; Lu, P.; et al. The chemistry and promising applications of graphene and porous graphene materials. *Adv. Funct. Mater.* **2020**, *30*, 1909035. [[CrossRef](#)]
72. Backes, C.; Abdelkader, A.M.; Alonso, C.; Andrieux-Ledier, A.; Arenal, R.; Azpeitia, J.; Balakrishnan, N.; Banszerus, L.; Barjon, J.; Bartali, R.; et al. Production and processing of graphene and related materials. *2D Mater.* **2020**, *7*, 022001. [[CrossRef](#)]